Soft Comput (2013) 17:29–37
DOI 10.1007/s00500-012-0898-1

ORIGINAL PAPER

Carlisle 2005 urban flood event simulation using cellular automata-based rapid flood spreading model

Yang Liu · Gareth Pender

Published online: 20 July 2012

Abstract In this study, we propose a new method to apply the rapid flood spreading model (RFSM) using cellular automata (CA) to multiple inflows of Carlisle, UK. The purpose of the RFSM is to generate predictions of water depth and flood extent using less computer resource than required by two-dimensional shallow water equation models (SWEMs). To be useful the RFSM must produce predictions that are comparable with those obtained from SWEMs. This paper reports a validation data available to the date on an urban flood, collected in January 2005 after a major event in the city of Carlisle, UK. This demonstrates an agreement between the proposed RFSM and measured data.

Keywords Cellular automata · Rapid flood spreading model · Shallow water equation model · Urban flood

1 Introduction

Two-dimensional (2D) hydrodynamic models have found a wide range of application in various fields of science and engineering. This has been supported by the increasing availability of remotely sensed digital elevation data and the growth in computing power. They are considered to give a good description of the hydraulic processes since they cater for both mass and momentum conservation. Despite the great success achieved in real-world applications, 2D models have also encountered many challenges. For a 2D model, a higher computational cost is needed when applied to a high-resolution grid. In many real-world applications, simulation time is not trivial. There are several situations in which the computational resources of 2D models become prohibitive and computational efficient flood inundation models have to be adopted. Lhomme et al. (2008) reported that flood risk analysis involves the integration of a full range of loading, multiple defence system states and uncertainty related to the input parameters of the 2D model and this type of analysis needs thousands of simulations of flood events. The expense of 2D models makes it unfeasible to generate predicted flood extents arising from hundreds of combination of entry points and floodwater volumes. Although the use of parallel computing offers a potential remedy to these problems in reducing the overall computational time, an alternative method of using fast inundation models to replace computationally expensive model evaluations has been suggested recently (Néelz et al. 2007; Krupka et al. 2007).

The concept of fast inundation models relies heavily on replacing time-consuming simulation models with a simplified model structure that is much faster but retains sufficient accuracy upon which to base suitable decisions. The requirements of RFSMs are therefore fast computation linked to sufficient accuracy and numerical robustness. Evaluation of RFSMs is normally based on two criteria: (1) a good overall agreement of the water depth and (2) a good overall agreement of the flood extent when compared with SWEMs. The use of fast models has only recently (Krupka et al. 2007; Lhomme et al. 2008; Liu and Pender 2010; Liu et al. 2009) become a topic of interest. Krupka et al. (2007), Liu and Pender (2010) and Lhomme et al. (2008) developed three similar rapid flood spreading

Y. Liu (✉)
Department of Engineering, Edinburgh University, Edinburgh EH9 3JL, UK
e-mail: sharkyangliu@gmail.com

G. Pender
School of the Built Environment, Heriot-Watt University, Edinburgh EH14 4AS, UK

models (RFSMs) using a heuristic kind algorithm, called cellular automata (CA). The CA has attracted much attention and has been widely applied to problems in almost all research fields in the past two decades (Guo et al. 2007). The CA has attracted much attention and has been widely applied to problems in almost all research fields in the past two decades (Guo et al. 2007). Krupka (2008) proposed a rapid one-direction spilling flood inundation model. The model was divided into two parts: in pre-calculation, an array of flood storage cells is constructed from a digital elevation map (DEM) of the flood risk area. In the inundation routine, a specified volume of flood water is distributed across the storage cells. The water will spread from a cell to its lowest neighbour with a constant driving head. The spatial measure of fit and the RMSE of flood depth prediction were used to evaluate the performance between a more complex hydrodynamic model (TUFLOW) and the RFSM. The spatial measure of fit gives the percentage agreement in flood prediction and RMSE gives an indication of agreement in flood depth prediction in these flood cells. The rapid simulation undertaken for the Thames mead site took less than one second. Similar flood extent predictions to those by TUFLOW were obtained as long as a reasonable estimate of constant extra head is used (Krupka 2008). Liu and Pender (2010) described an improvement on the previous RFSM as it dynamically adjusts the head driving the flood flow to account for the rate of flood inflow and the frictional resistance of the floodplain. This allows the RFSM to adapt predictions of inundation extent to surface characteristics to the area over which the water is spreading. Improvements in this technique have been applied to the same catchment. This demonstrates that the method significantly improves the level of agreement between the proposed RFSM and a SWEM when compared with the performance of a previous spreading algorithm. Similarly, Lhomme et al. (2008) described improvements to the rapid flood spreading model that focused on incorporating additional physical process within the spreading algorithm (multiple spilling and friction). This improved model was applied to a number of different sites (Carlisle, Cumbia, UK; River Brit, Dorset, UK; Boston, East Anglia, UK; River Lee, London, UK) and compared well with simulations obtained using the TUFLOW. The mean deviation, the fit and bias of predicted depths were used to evaluate performance by quantifying the matching of the flood extent from both models. These test results suggested that the RFSM was capable of producing comparable predictions using a computationally less expensive technique (run time typically <5 s). In particular, they reported that incorporation of multiple spilling and friction effects in the algorithm had a significant benefit in improving the model predictions for flat floodplains.

Recently, the attention of flood inundation modellers has focused on more complex urbanized catchments, where the value of assets at risk is greater (Neal et al. 2009). However, instances where the accuracy of the proposed RFSM simulation has been assessed against field observations of inundation extent or water surface elevation are rare to date, due to lack of validation data. Inundation extent data in urban areas are rare because it is difficult to obtain high-resolution imagery that coincides with the flood peak. The aim of this paper was to assess the predictability of rapid flood spreading model using cellular automata and present a test case for model validation in urban areas. In addition, we propose a new method to apply the RFSM to multiple inflows of Carlisle, UK.

2 Rapid flood inundation model using cellular automata

2.1 Basic algorithm

Cellular automata are spatially and temporally discrete dynamic systems characterized by local interaction, self-production and universal computation (Chopard and Droz 1998). A standard cellular automaton consists of a regular grid of cells, each in one of a finite number of states. At every modelling step, the states of all cells are updated synchronously by an identical set of transition rules. For each cell, the updating only involves the previous state of the cell and of its predefined neighbours. Despite the simple principles of cellular automata, very complex behaviours can be generated (Guo et al. 2007). The rapid flood spreading model consists of two parts: (1) a pre-calculation routine, in which an array of flood storage cells is constructed from a digital elevation map (DEM) of the flood risk area; and (2) an inundation routine, in which a specified volume of flood water is distributed across the storage cells (Krupka et al. 2007). The pre-calculation process identifies low points on the DEM and expands these outwards in a manner similar to a growing area of ponded water. The size and number of storage cells are controlled by two flood cell parameters—the minimum area of a flood cell and the minimum depth of a flood cell. Thus by varying these limits the terrain can be represented at several different spatial resolutions ranging from very many small pools to very few large pools. Once the flood risk area is covered with viable cells, links (potential flow paths) between neighbouring cells are identified by searching for the lowest elevations on the inter-cell boundaries. Finally, volume-elevation curves are constructed for each cell from its topography, for use in the inundation routine. Figure 1 shows the expansion process. In inundation routine, the water will spread from a big cell

to its lowest neighbour with a constant extra head (see Fig. 2). The entry point of the water to the flood risk area and the total volume of flood water to be spread are determined by the modeller. The inundation calculation begins by filling the cell containing the entry point. When the lowest link to a neighbouring cell is reached, the entry cell stops filling and the neighbouring cell fills until its water level reaches its lowest link, at which point the next cell begins to fill (see Fig. 3). This process continues until all the floodwater has been transferred to cells. A pseudo-code version of the standard one-directional spilling RFSM algorithm is shown below:

- *Initialize the four parameters*: the minimum cell plan area (Amin), minimum cell depth (Dmin), total volume of water for spreading (total_volume) and constant driving head Δ_z.

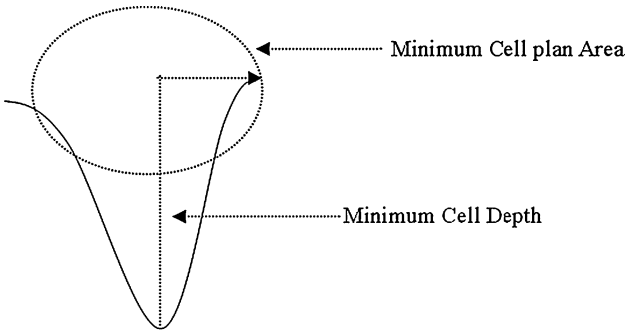

Fig. 1 An example of expansion process

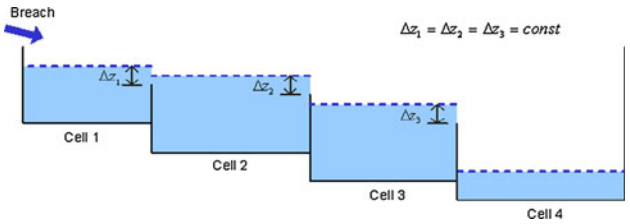

Fig. 2 An example of a flood distribution

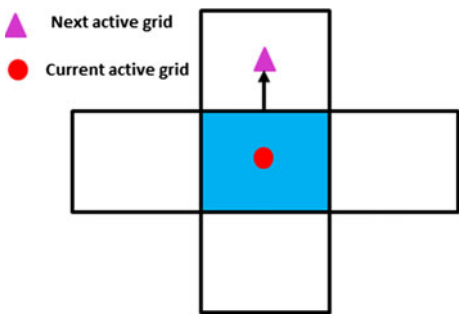

Fig. 3 One-directional spilling process

- Divide the big floodplain into the small number of n big flood cells based on two parameters Amin and Dmin.
- Save the water level versus volume for each big flood cell in a file and its neighbours and link water levels of its neighbours.
- Set the volume_sum = 0.
- Set the start location for spreading and the current flood cell becomes active.
- Boolean (i) = 1//start big flood cell becomes active.
- Set the water level for each big flood cell = its lowest digital elevation data.
- Do while (volume_sum < total_volume).
- Find the next active grid based on current active cell's neighbour's water level data.
- Next active index = p.
- Set current active flood cell water level:
- If the current flood cell is dry (Boolean (i) = 0) then.
- Water_level (i) = water level of its lowest link level + driving head.
- Else the current flood cell is wet (Boolean (i) = 1).
- Water_level (i) = water_level (i) + driving head.
- Endif.
- Volume_sum = volume_sum + current_volume// record the volume of water that has been spread so far.
- Endwhile.

A simple artificial test terrain is used to demonstrate the CA algorithm. The domain in Fig. 4a consists of six depressions that have been identified by the precalculation routine. All compartments have plan areas of 20,000 m^2, flat bottoms at a level of 10.0 metres and are separated from their neighbours by walls. The elevation of the inter-cell walls, which act as the links between cells are depicted in Fig. 4a. A wall also surrounds the whole domain having a crest at a level of 15.0 m, which ensures no water is allowed to leave the domain. A flood incident resulting in the flooding of cell 3 is simulated. The total volume of inundation, which in a real scenario would be calculated from an inflow hydrograph, is set at 55,000 m^3. The extra head value Δ_z of 0.3 m considered. The calculation starts at cell 3 (Fig. 4b), which is filled up to the level of the lowest link (10.3 m) plus the extra head value (+0.3 m), because cell 2, which will be linked in the next step, is dry. Cell 2 is activated (Fig. 4c). The water level rises to the level of the lowest link, which is the link back to the cell 3. The extra head value is not added to cell 2, because cell 3 has already been flooded. Figure 4d shows the next step in which both cells 2 and 3 are active. The next lowest link is at the level of 10.4 m to cell 5. The extra head is applied to both active cells, because cell 5 is dry. Depths in cells 2 and 3 then rise to 0.7 m. Next, cell 5 is active while cells 2 and 3 are inactive (Fig. 4e). There are two lowest links from cell 5 to 4 and to cell 6, which are both dry; hence, the extra head is

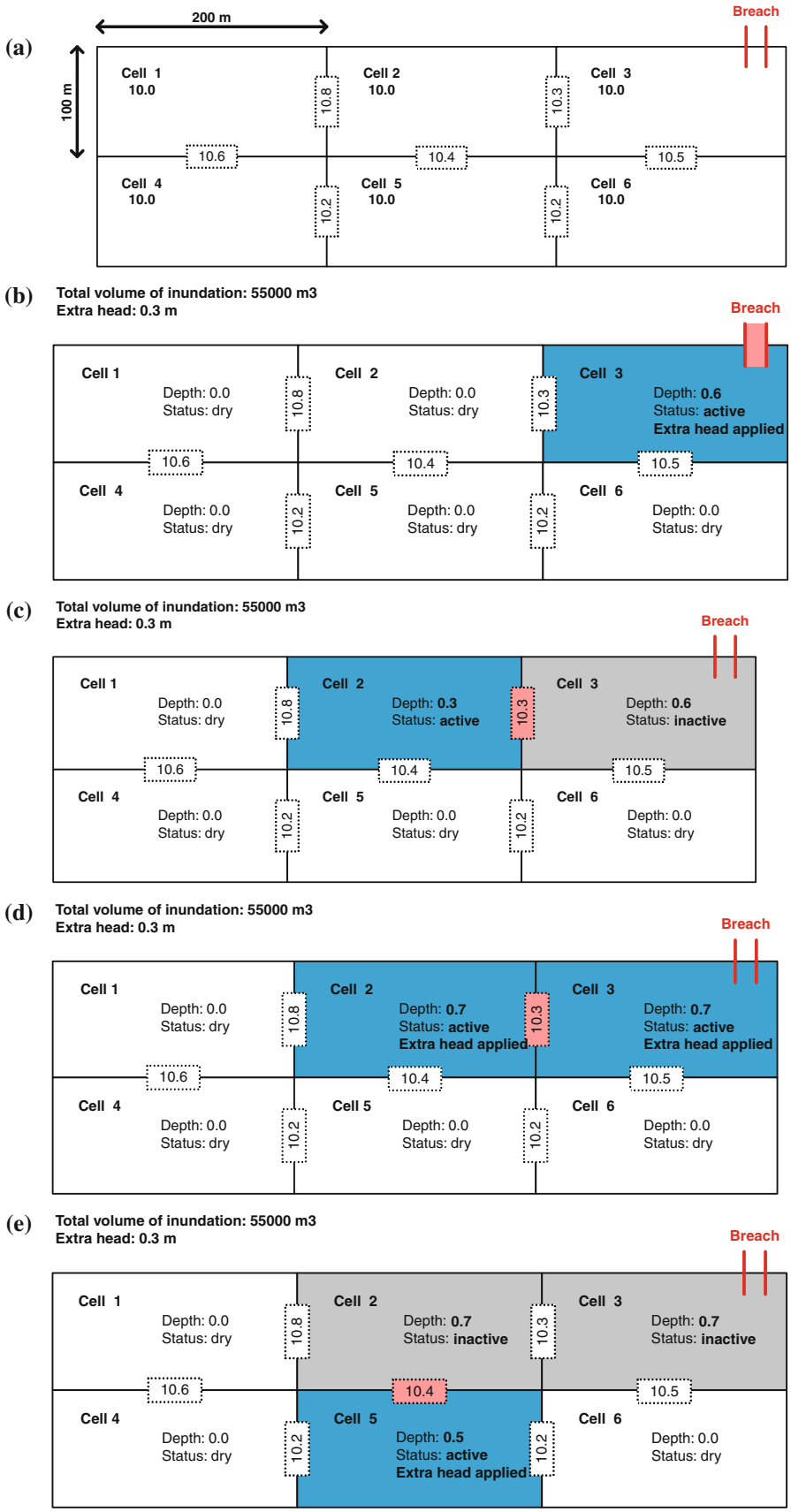

Fig. 4 CA iteration process

Fig. 4 continued

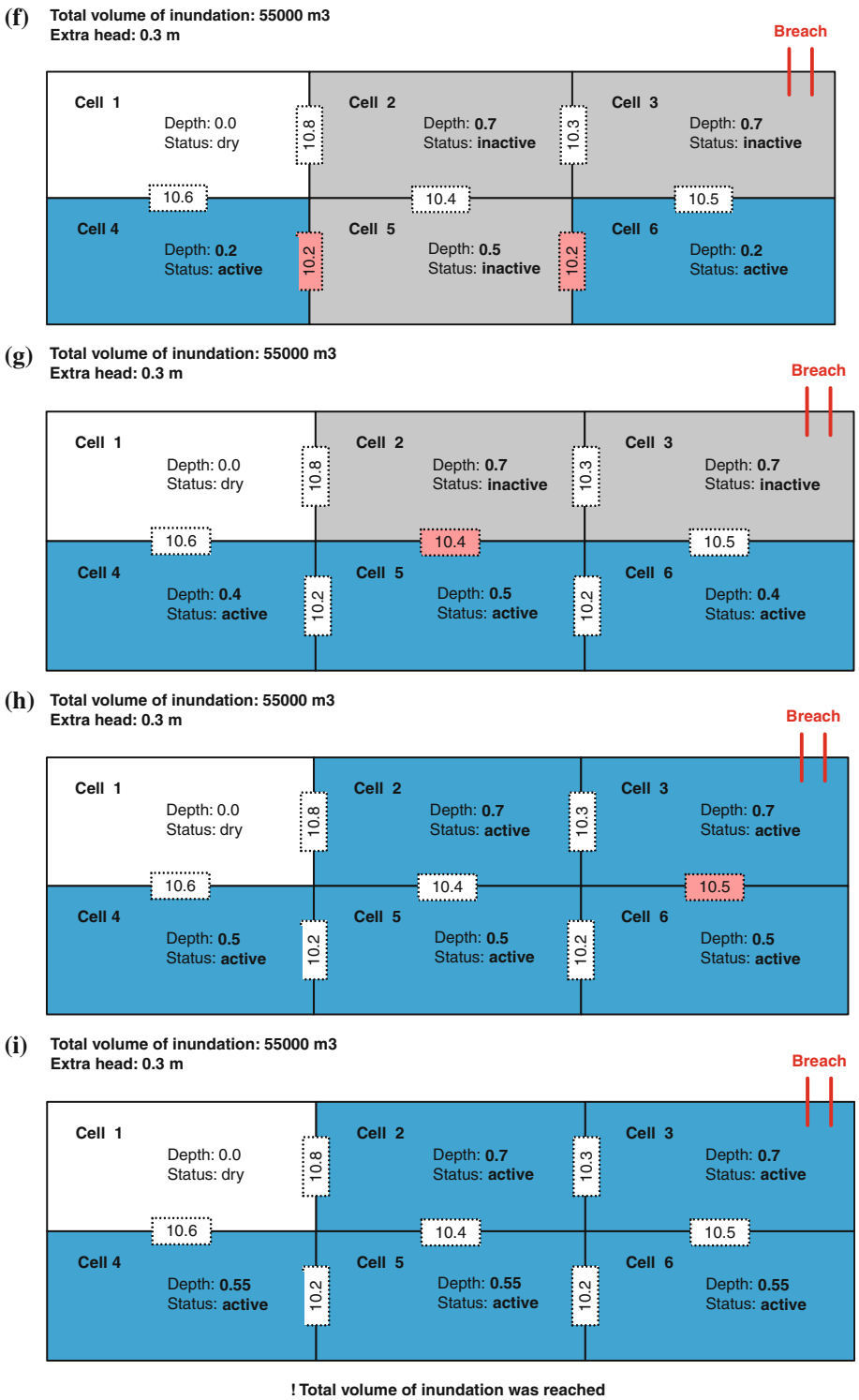

applied to cell 5 and the depth in this cell increases to 0.5 m. In Fig. 4f, cells 4 and 6 become active. The lowest links from these cells lead back to cell 5, which is already flooded. Hence no extra head is applied to cell 4 and 6. All three cells 4, 5 and 6 are now active. The lowest link from these three cells leads back to cell 2, which has been flooded before—no extra head is applied to cells 4, 5 and 6 (Fig. 4g). However, the depths in cell 4 and 6 increase to 0.4 m. In the next step, cells 2 and 3 also become active (Fig. 4h). Now the lowest link from all active cells is the internal link between cells 3 and 6, which both have already been flooded; hence no extra head is applied.

Table 1 RFSM parameters

Model parameters	Description	Lower bound	Upper bound
Amin	Minimum cell plan area (m^2)	500	50,000
Dmin	Minimum cell depth (m)	0.1	2
Δ_z	Constant driving head for RFSM (m)	0.001	2

The water level is increased only in cells 4 and 6 to the depth 0.5 m so they reach the level of the current lowest link (10.5 m between cells 3 and 6). The total volume check is applied to stop the calculation when all the available volume has been spread. Figure 4i shows that the water level has been iterated and rose to give a depth of 0.55 m in cells 4, 5 and 6. It should be stressed that Fig. 4i depicts maximum depths experienced by every cell during the inundation, not the final depths. A realistic Δ_z parameter value needs to be selected to well represent the real event. No guidance on this parameter value is available in the literature; hence the model needs to be calibrated to find optimum value (Krupka 2008).

2.2 The proposed method for multiple inflows of RFSM using CA

Here, we propose a new method to apply the RFSM using CA to multiple inflows problem:

1. We set the main inflow location as the spreading location using the RFSM. This is because the flooding is predominantly the result of overflow from the main river.
2. The different constant driving head values of flood cells are adjusted to get a good prediction.

In this paper, we will test prediction accuracy of the proposed method to Carlisle, UK, with three inflows compared with a SWEM (ISIS2D) and measured data.

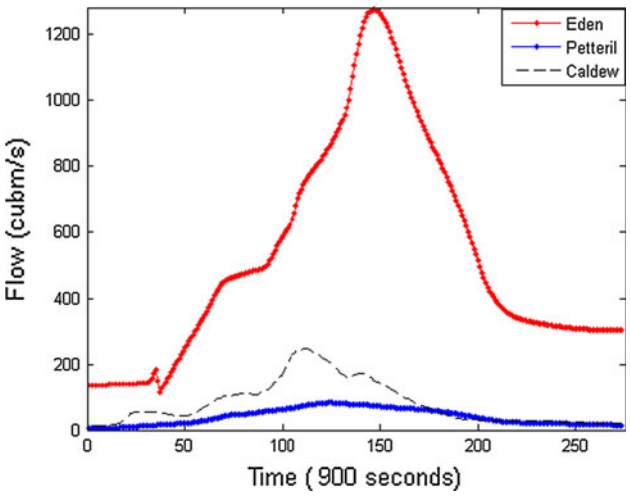

Fig. 6 Inflows to Carlisle model from the Rivers Eden, Petteril and Caldew

3 Model parameters and objective functions

A brief description of calibration parameters used is given in Table 1. In order to evaluate the performance of the RFSM, it is necessary to formulate numerical performance measures that reflect the different objectives. Two objective functions (each corresponding to the goodness-of-fit criteria) are formulated as follows:

$$F_1(\theta) = \frac{\mathrm{Num}\left(S_{\mathrm{RFSM}} \cap S_{\mathrm{2DModel/Obs}}\right)}{\mathrm{Num}\left(S_{\mathrm{RFSM}} \cup S_{\mathrm{2DModel/Obs}}\right)} \quad (1)$$

$$F_2(\theta) = \mathrm{MAE} = \frac{1}{n}\sum_{i=1}^{n}\left|h_{\mathrm{2dmodel}_i/\mathrm{Obs}_i} - h_{\mathrm{RFSM}_i}\right| \quad (2)$$

where the Num function gives the number of members of the set, S_{RFSM} and $S_{\mathrm{2DModel/Obs}}$ represent the sets of pixels classified as wet by the rapid flood inundation model and by SWEM or observed data, respectively, and i is the i'th pixel of the domain consisting of n pixels. The numerator

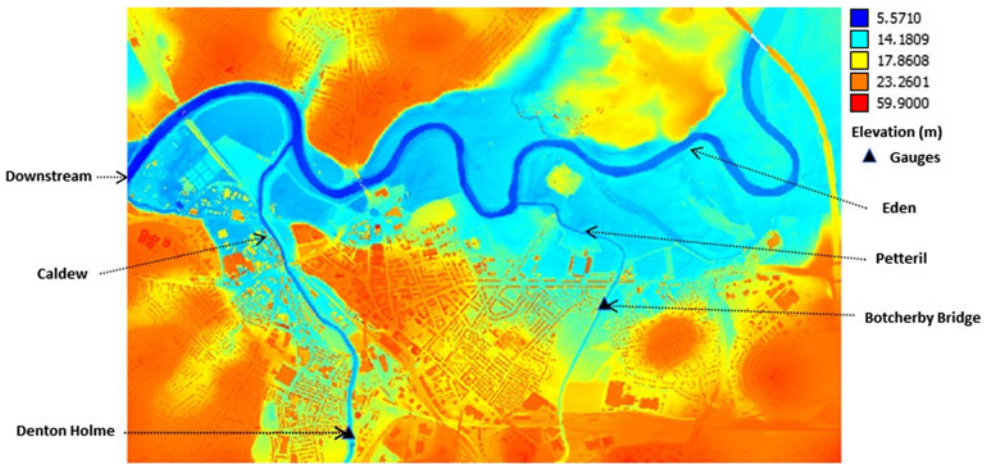

Fig. 5 5 m grid resolution digital elevation data of Carlisle, UK and two gauges (Botcherby Bridge and Denton Holme)

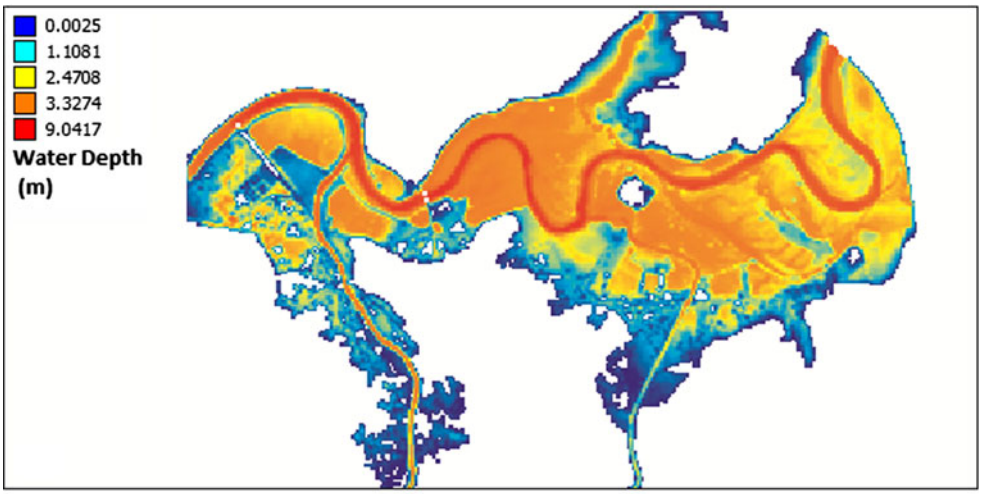

(a) Flood extent and water depth (m) after 45.25 hours using ISIS2D.

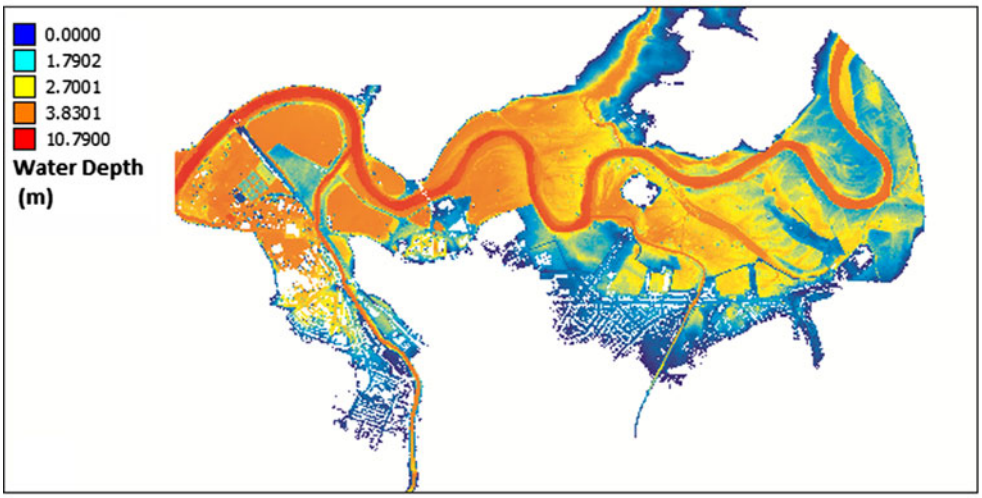

(b) Flood extent and water depth (m) at 45.25 hours using RFSM.

Fig. 7 Flood extents of Carlisle using ISIS2D and RFSM at peak volume on the floodplain

represents the intersection of the two flood extent maps while the denominator represents their unification. In case of total agreement of flood extents, F_1 would become equal to 1, while in case of zero agreement F_1 would be 0. The higher the F_1 value, the better predictor of the flood extent the parameter set is. The F_2 assesses the quality of water depth prediction in these pixels. Therefore, the second measure is used—a mean absolute error (MAE) of the flood depth predictions compared with a SWEM result, where h_{RFSM_i} and $h_{2\mathrm{dmodel}_i/\mathrm{Obs}_i}$ are predicted water depths in the i'th pixel in rapid flood inundation model and the SWEM or observed data. The lower the MAE value, the better the agreement between the SWEM and RFSM predictions. The development of flood risk analysis has focused mainly on the selection of a single objective measure of flood extent and water depth. However, practical experience with hazard analysis suggests that no single-objective function is adequate to measure the ways in which the model fails to evaluate the important characteristics of the observed data. In order to successfully measure flood hazard of a 2D model, multiple criteria should be considered.

4 Experiment setup and result

The RFSM was tested on the Carlisle floodplain, in UK. The Environment Agency of England and Wales (EA) provided a digital surface model (DSM) of the study site, generated from an airborne laser altimetry (LiDAR) survey undertaken in March 2002 and updated along the River Caldew in November 2005. These data were post-processed by Mason et al. (2007) to produce a digital elevation model (DEM) (Fig. 5) that includes buildings but not vegetation and a digital terrain model (DTM) without buildings or vegetation. Simulations obtained from a

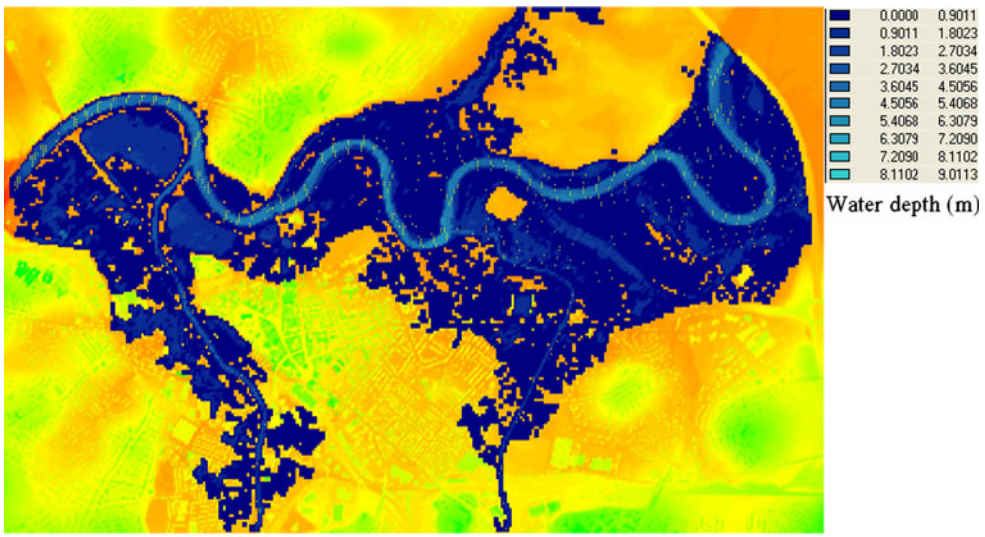

Fig. 8 Final flood extent and water depth using ISIS2D after 72 h

SWEM (ISIS2D) and measured data were therefore used as the basis of comparison. The study case was modelled using ISIS2D. At the core of ISIS2D, there are two solution methods that are specifically developed to tackle different types of hydraulic conditions: alternating direction implicit (ADI) and total variation diminishing (TVD) finite difference schemes. We choose to run a 15-m grid model for the experiment using ISIS2D with ADI method. A value of Manning's $n = 0.05$ was used in river channels and $n = 0.04$ was used on floodplain. The computational time was about 1 h for the 15-m grid model (with 1 s time step) on an Intel core 2 Quad CPU 2.83 GHz and 3 GB of RAM. The hydrographs for each river are shown in Fig. 6. It was assumed that all flow entered the model domain via these river channels. Flow was allowed to leave the domain as a free surface flow just west of the floodplain, shown in Fig. 5.

Table 2 Performance statistics using RFSM

Flood extent prediction of peak volume of water using RFSM	
MAE	0.25
Fit	86.28 %

The start of spreading location is the upstream of Eden River using RFSM (see Fig. 5). This is because the flooding is predominantly the result of overflow from the main river. Figure 7a, b shows flood extent predictions of peak volume of water obtained using ISIS2D compared with the RFSM, and Fig. 8 shows final flood extent prediction on the floodplain using ISIS2D. The risk is the greatest of peak volume of water on the floodplain for the flood risk analysis, so we calculate the performance statistics of Fit and MAE for the flood extent prediction of peak volume of water is shown in Table 2. The RFSM is been shown to compare well against ISIS2D for the Carlisle, producing the prediction of flood extent in a significantly shorter run time (typically <2 s) but there is about 0.25 m difference of water depth prediction between the RFSM and ISIS2D based on MAE measure. In order to measure the prediction accuracy of the RFSM and ISIS2D, we compared their water level predictions with measured data in two gauge stations (Botcherby Bridge and Denton Holme) in Fig. 5. With respect to the AE measures in Table 3, the RFSM using CA has a better performance compared with ISIS2D. The large difference between ISIS2D prediction and measured data could because the coarse grid data (15 m resolution grid) was used to get quick running time (about 1 h) on the single PC for the

Table 3 Performance statistics of peak volume

Test locations	Measured data (m)	Water level using RFSM (m)	Water level using ISIS2D (m)
Botcherby Bridge	16.002	16.1330	16.57716
AE between measured data and RFSM/ISIS2D for Botcherby Bridge		0.1310	0.5752
Denton Holme	15.2920	16.1350	16.6091
AE between measured data and RFSM/ISIS2D for Denton Holme		0.8430	1.3171

long simulation period (around 72 h). The most sensitive parameter of RFSM is minimum cell depth using local Morris method (Liu and Pender 2010; Morris 1991). The model parameters (Amin, Dmin, Δ_z) need to be calibrated using the multi-objective optimisation algorithms for a real application (Liu and Pender 2011). The optimal parameters (Amin = 6,000, Dmin = 0.6 and $\Delta_z = 0.6$) were obtained after calibration. For a more detailed description of automatic calibration and its applications the reader is referred to Liu (2009).

5 Conclusions

Simulating flood inundation problems usually requires a large amount of computation time for high-resolution data. The focus of this research was to develop a fast inundation model that produced predictions comparable with those obtained from 2D shallow water equation models or observations. The RFSM using CA has been applied to multiple inflows of Carlisle, UK. This experiment showed that the water depth and flood extent predictions obtained were comparable to measured data and ISIS2D simulated results. The evaluation scheme considers numerical performance measures of two different objectives: (1) flood extent and (2) water depth. Work is currently undergoing to include (1) velocity prediction and (2) multi-objective calibration in the RFSM.

Acknowledgments The research reported in this paper was conducted as part of the Flood Risk Management Research Consortium. The FRMRC is supported by Grant EP/F020511/1 from the Engineering and Physical Sciences Research Council, in partnership with the DEFRA/EA Joint Research Programme on Flood and Coastal Erosion Risk Management, UKWIR, OPW (Ireland) and the Rivers Agency (Northern Ireland). This financial support is gratefully acknowledged. The authors are also grateful to Environment Agency for providing LiDAR the data and the Ordnance Survey for providing Mastermap® data. The comments and advice received from Julian Lhomme, HR Wallingford Ltd. are also acknowledged.

References

Chopard B, Droz M (1998) Cellular automata modelling of physical systems. Cambridge University Press, UK

Guo YF, Keedwell E, Walters G, Khu ST (2007) Hybridizing cellular automata principles and NSGAII for multi-objective design of urban water networks. In: Proceedings of the 4th international conference on evolutionary multi-criterion optimization, vol 4403, Matsushima, Japan, 5–8 Mar 2007, pp 546–559

Krupka M (2008) A rapid inundation flood cell model for flood risk analysis. PhD thesis, Heriot-Watt University, Edinburgh

Krupka M, Wallis S, Pender G, Neélz S (2007) Some practical aspects of flood inundation modelling, Transport phenomena in hydraulics. Institute of Geophysics, Polish Academy of Sciences, E-7(401): 129–135

Lhomme J, Sayers P, Gouldby B, Samuels P, Wills M, Mulet-Marti J (2008) Recent development and application of a rapid flood spreading method. River Flow 2008:15–24

Liu Y (2009) Automatic calibration of a rainfall-runoff model using a fast and elitist multi-objective particle swarm algorithm. Expert Syst Appl 36(5):9533–9538

Liu Y, Pender G (2010) A new rapid flood inundation model. In: proceedings of the first IAHR European Congress, 4–6 May 2010, Edinburgh

Liu Y, Pender G (2011) Optimal parameter estimation of a rapid flood spreading model using multi-objectives. In: Proceedings of the 34th IAHR 2011 Congress, 21 June to 1 July 2011, Brisbane, pp 256–263

Liu Y, Neélz S, Pender G (2009) Improving the performance of fast inundation models using v-support vector regression and particle swarm optimisation. In: Proceedings of the 33rd IAHR 2009 Congress, Vancouver, pp 1436–1443

Mason DC, Horritt MS, Hunter NM, Bates PD (2007) Use of fused airborne scanning laser altimetry and digital map data for urban flood modelling. Hydrol Process 21:1436–1447

Morris MD (1991) Factorial sampling plans for preliminary computational experiments. Technometrics 33:161–174

Neal JC, Bates PD, Fewtrell TJ, Hunter NM, Wilson MD, Horritt MS (2009) Distributed whole city water level measurements from the Carlisle 2005 urban flood event and comparison with hydraulic model simulations. J Hydrol 368:42–55

Néelz S, Hall J, Pender G (2007) Improving the performance of fast flood inundation models by incorporating results from very high resolution simulations. In: Proceedings of flood risk assessment II conference, Institute of Mathematics & its Applications, Southend on Sea, pp 1–9